united nations
educational, scientific
and cultural
organization

international atomic
energy agency

the
abdus salam
international centre for theoretical physics

H4. SMR/1247
Lecture Note: 05

WORKSHOP ON PHYSICS OF MESOSPHERE-STRATOSPHERE-TROPOSPHERE INTERACTIONS WITH SPECIAL EMPHASIS ON MST RADAR TECHNIQUES

(13 - 24 November 2000)

FIRST D-REGION INCONHERENT SCATTER AND PMSE OBSERVATIONS WITH THE EISCAT SVALBARD RADAR (500MHz) AND COMPARISON WITH PMSE OBSERVED WITH THE COLLOCATED SOUSY SVALBARD RADAR (53.5 MHz)

Prof. Jurgen ROTTGER

Max-Planck-Institut fur Aeronomie
Katlenburg-Lindau
GERMANY

strada costiera, 11 - 34014 trieste italy - tel. +39 40 2240111 fax +39 40 224163 - sci info@ictp.trieste.it - www.ictp.trieste.it

First D-region incoherent scatter and PMSE observations with the EISCAT Svalbard Radar (500 MHz) and comparison with PMSE observed with the collocated SOUSY Svalbard Radar (53.5 MHz)

Jürgen Röttger
Max-Planck-Institut für Aeronomie
D-37191 Katlenburg-Lindau, Germany
<roettger@linmpi.mpg.de>

The EISCAT Svalbard Radar (ESR) is an incoherent scatter radar for studies of the polar ionosphere and the magnetosphere (Röttger et al., 1995). First applications of the ESR, using special experiment codes for mesosphere and D-region observations were described by Röttger et al. (1998). The SOUSY Svalbard Radar (SSR) is an MST radar, which was particularly established for observations of Polar Mesosphere Summer Echoes (PMSE). It is briefly described by Czechowsky et al. (1998). An update of the SSR system and particular observations of PMSE and the lower stratosphere and troposphere is found in the companion papers by Röttger et al. (2000) and Röttger and Trautner (2000). Fig. 1 shows photos of the antennas of the ESR and SSR. As shown on the map in Röttger et al. (2000), both radars are located very close to each other, which allows simultaneous and real common volume observations of the middle atmosphere.

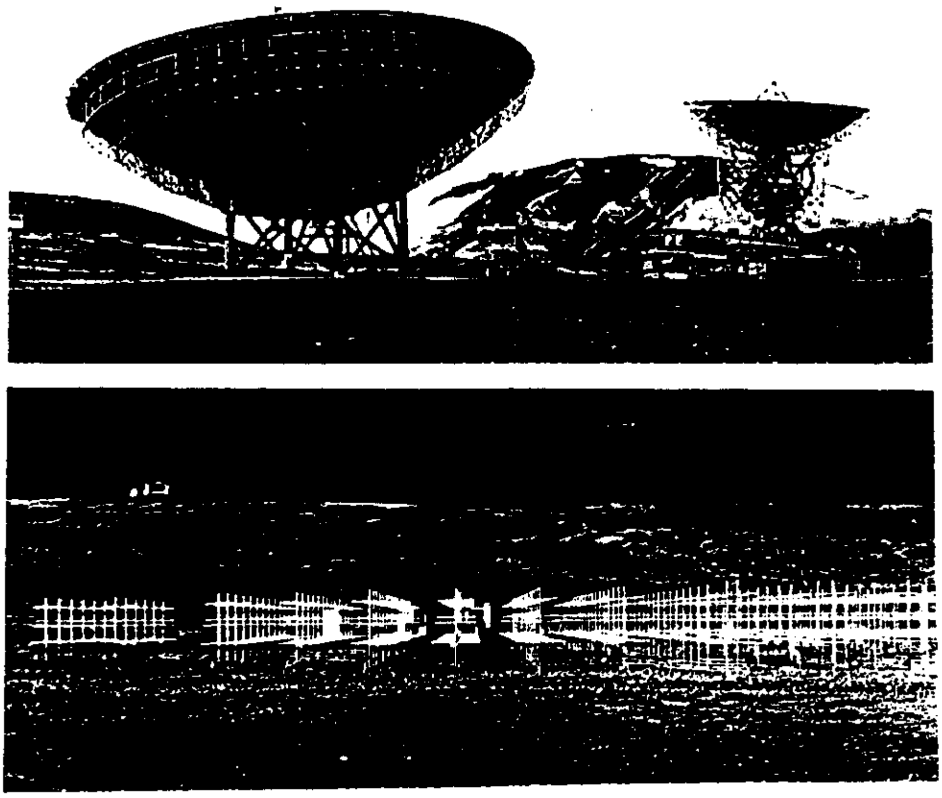

Fig. 1 The 42-m and 32-m antennas of the EISCAT Svalbard Radar (upper photo). For the observations presented in this paper the steerable 32-m antenna was used. The lower photo shows part of the steerable phased array antenna of the SOUSY Svalbard Radar, which consists of 356 Yagi antenna elements.

To appear in:
Proceedings of the Ninth Workshop on Technical and Scientific Aspects of MST Radar, ed. B. Edwards, SCOSTEP, Boulder, USA, 2000.

J01

The main system parameters of the EISCAT Svalbard Radar (ESR) and the SOUSY Svalbard Radar (SSR) are given in Table 1. Both radars were operated with complementary codes. In the beginning of the ESR operations with the standard alternating code modulations, observations of the E- and D-region were impossible due to the very strong ground clutter. This has been ameliorated by a modified scheme where signals from subsequent interpulse periods are subtracted (Van Eyken et al., 2000). It turns out that the particular method of ground clutter removal, as applied with MST radars, works superior, in particular for observations of the D-region below about 88 km, and of PMSE up to above 92 km, since these have much narrower spectra than the incoherent scatter signals from that altitudes. First results using this technique for D-region incoherent scatter observations with the ESR are found in Röttger et al. (1998).

SYSTEM PARAMETERS	ESR	SSR
Antenna gain G in dBi	42.5	33.0
Half power beam width Θ	1.23°	4.0°
Frequency f in MHz	500	53.5
Wavelength λ in m	0.60	5.61
Peak power P_p in MW	0.8	0.07
Duty cycle d	0.14	0.04
Average power P_a in kW	115	2.8
Number n_b of code bauds	32	20
Effective power $2 \cdot P_p \cdot n_b$ in MW	51.2	2.4
System efficiency (assumed)	0.8	0.8
Pulse (baud) length τ in μs	6	2
System temperature T_s in K	70	3000
Number coherent integrations n_{coh}	2	4x21
Detection bandwidth f_b in kHz	83.3	2.98
System figure of merit F_m	$1 \cdot 10^{23}$	$6 \cdot 10^{22}$
Minimum detectable radar reflectivity η in m^{-1}	$2.6 \cdot 10^{-19}$	$7.5 \cdot 10^{-19}$

Table 1

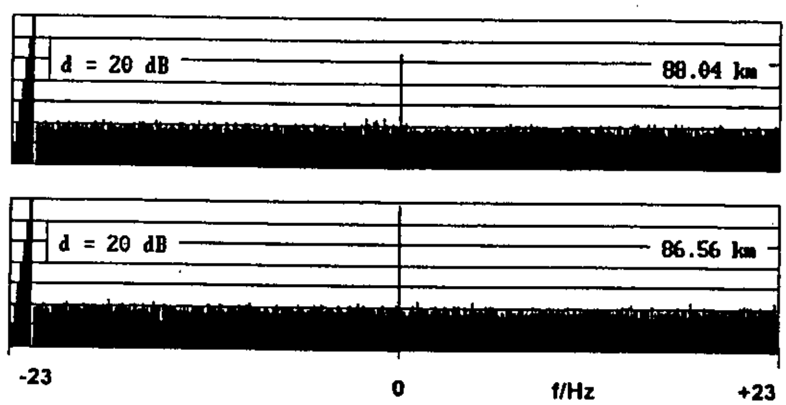

Fig. 2 Power spectra of ranges where PMSE are expected to occur. The Nyquist freqency is 23.148 Hz and the spectral resolution 0.090 Hz. These 512-point spectra result from 48 incoherent integrations over a period of 66.355 s.

Since PMSE usually have much narrower spectra than the incoherent scatter signals, we have to assure in this case that the ground clutter echoes have a much narrower spectral widths than even those of PMSE. To check this, spectra of signals from ranges around 80 km to 90 km were analyzed with a very high frequency resolution. Fig. 2 shows such high resolution spectra. The ground clutter is confined to the spectral bin at 0 Hz and has a signal-to-noise ratio of up to 50 dB within the narrow bin of 0.090 Hz. There are no sidebands noticed, which means that phase or amplitude changes of ground clutter echoes are at time scales of much less than10 seconds, if they occur. This result is regarded very satisfying for the presented D-region and PMSE observations with the ESR. The weak enhancement of spectral power around -2 Hz

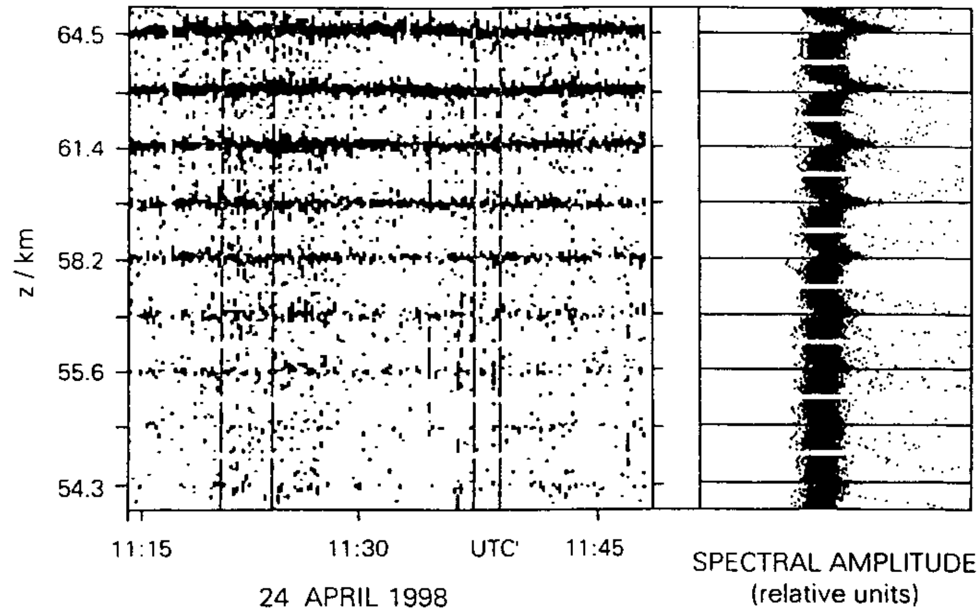

Fig. 3 Incoherent scatter signals observed with the EISCAT Svalbard Radar. The panels show spectra of signals in 9 range gates at altitudes between 54.3 km and 64.5 km, where the echoes are getting stronger with increasing altitude. The zero frequency is indicated by the tick marks and the solid lines in the right-hand panel. The Nyquist frequency is ± 33 Hz. Incoherent scatter echoes can be seen down to the lowest range gate. The vertical lines are either due to meteor echoes (code sidebands) or satellites.

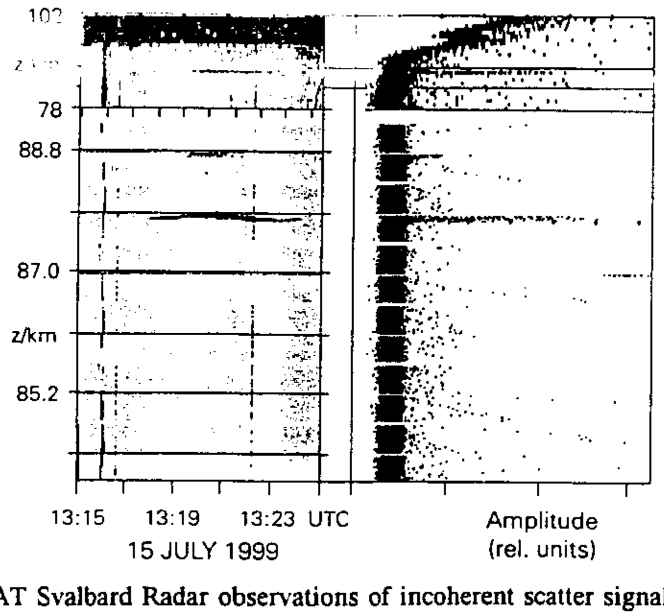

Fig. 4 EISCAT Svalbard Radar observations of incoherent scatter signals from the lower E-region (> 90 km) and coherent scatter due to PMSE (87.9 and 88.9 km): Amplitude scatter plots in the upper right-hand corner. In the upper left-hand side the corresponding height-time intensity plot is shown. The two lines indicate the ranges of which dynamic spectra and spectra scatter plots (lower panels) are displayed. The continuous line in the dynamic spectra is at 0 Hz. The corresponding frequency bin in the spectra scatter plots is empty, since the ground clutter is much larger than the noise level.

is due to PMSE (Fig. 2). That signal is clearly wider than the clutter line. However, there may be different weather conditions, which may cause phase path changes resulting in a spectral widening of the ground clutter. This would require further observations. Fig. 3 shows dynamic shows dynamic spectra of incoherent scatter echoes and the corresponding scatter plots of the spectral amplitudes, recorded over a period of 32 minutes. This was during the recovery phase of a solar proton event, which had increased the D-region electron density, such that echoes could be detected down to about 55 km. In Fig. 4 a similar display is shown for quiet ionosphere conditions. The height-time intensity and the scatter plots in the upper panels display the increase in echo amplitude above about 88 km, which is due to incoherent scatter from the lower E-region, which even shows an indication of a thin (sporadic?) E-layer just below 100 km. The dynamic spectra in the left-hand lower panels show that there are clear spectral lines at ranges 87.9 km and 88.8 km. These repeat in the spikes in the scatter spectra plots on the lower right-hand plots. These spikes and spectral lines are clear indicators of PMSE. The amplitude of these coherent scatter PMSE is comparable to the amplitude of the incoherent scatter signals from the lower E-region. The signal-to-noise ratio of the 500-MHz PMSE was observed in the order of 2 – 20 %. Hall and Röttger (2000) have done the statistics of these observations, which show a few percent occurrence frequency of PMSE. The signal power of the PMSE observed with the ESR is about 10^{-17} W, which can be converted into radar reflectivity. From the spectrum width (10 - 80 Hz at of the 500-MHz PMSE the turbulence energy dissipation rate is deduced to be in the order of 0.1 W kg^{-1}. An estimate of the background electron density of $5 \cdot 10^8$ m^{-3} is obtained from the incoherent scatter signals. Combining these quantities yields a radar reflectivity in the order of 10^{-19} m^{-1} on 500 MHz. Comparisons with simultaneous PMSE observations with the SSR (see Röttger et al., 2000), which yield radar reflectivities of 10^{-14} m^{-1} on 53.5 MHz, show a strong frequency dependence. Of course, these estimates are varying by about an order of magnitude, depending on the received signal power, the spectrum width, the assumed Brunt-Väisälä frequeny, and the electron density profile. Comparing these estimates, obtained at spatial scales an order of magnitude different, with calculations of Cho (1993) lead to the assumption that Schmidt numbers (determined by the electron diffusion coefficient) larger than 100 are needed to explain this scattering process. We conclude here that the electron diffusion in the polar summer mesopause is substantially reduced due to the presence of ice particles. More details on these evaluations and interpretations will be published in a more extended paper.

The author thanks his colleagues at MPAe for support on the SSR, and J. Markannen and C.M. Hall for support taking and analyzing ESR data. EISCAT is funded by CNRS, MPG, NFR, NIPR, RCN, PPARC and SA.

References:

Cho, J.Y.N., Radar Scattering from the Summer Polar Mesosphere: Theory and Observations, Ph.D. Thesis, Cornell University, Ithaca, New York, 1993.

Czechowsky, P., J. Klostermeyer, J. Röttger. R. Rüster and G. Schmidt, The SOUSY Svalbard Radar for middle and lower atmosphere research in the polar region, *Proc. 8th Workshop Techn. Scie. Aspects MST Radar*, SCOSTEP, 318-321, 1998.

van Eyken, A.P., P.J.S. Williams, S.C. Buchert and M. Kunitake, First measurements of tidal modes in the lower thermosphere by the EISCAT Svalbard Radar, *Geophys. Res. Lett., 27*, 931-934, 2000.

Hall, C.M., and J. Röttger, Initial observations of Polar Mesosphere Summer Echoes using the EISCAT Svalbard Radar, submitted to *Geophys. Res. Lett.*, 2000.

Röttger, J., U.G. Wannberg, and A.P. van Eyken, The EISCAT Scientific Association and the EISCAT Svalbard Radar Project, *J. Geomag. Geoelectr.*, 669-679, 1995.

Röttger, J., J. Markannen, and U.G. Wannberg, The EISCAT Svalbard Radar – Its potential for middle atmosphere studies, *Proc. 8th Workshop Techn. Scie. Aspects MST Radar*, SCOSTEP, 314-317, 1998.

Röttger, J., G. Schmidt, R. Rüster, P. Czechowsky, J. Klostermeyer, J. Trautner, K. Meyer, K.D. Preschel and H. Becker, An update on the SOUSY Svalbard Radar: Observations of Polar Mesosphere Summer Echoes, *Proc. 9th Workshop Techn. Scie. Aspects MST Radar*, SCOSTEP, this issue, 2000.

Röttger, J., and J. Trautner, Synoptic and meso-scale disturbances observed in the Artic troposphere and lower stratosphere with the SOUSY Svalbard Radar, *Proc. 9th Workshop Techn. Scie. Aspects MST Radar*, SCOSTEP, this issue, 2000.